

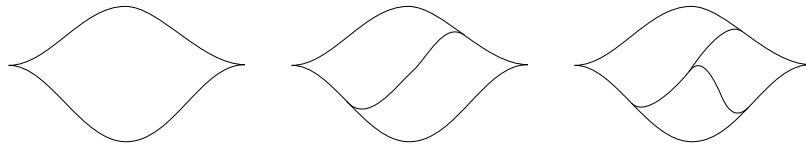
Arboreal singularities from Lefschetz fibrations

Vivek Shende

ABSTRACT. Nadler introduced certain Lagrangian singularities indexed by trees, and determined their microlocal sheaves to be the category of modules over the corresponding tree quiver. Another family of spaces indexed by trees: the tree plumbings of spheres. The Fukaya-Seidel category of the Lefschetz fibration with this plumbing as fiber and all spheres as vanishing cycles is well known to also be modules over the tree quiver. Here we upgrade this matching of categories to a matching of geometry.

1. Introduction

Fronts for Legendrian links of what Nadler calls the A_1, A_2, A_3 *arboreal singularities*:



More generally, there is an arboreal singularity for each tree. Each arboreal singularity is a singular Lagrangian. Those above correspond to the trees $\bullet, \bullet \rightarrow \bullet$, and $\bullet \rightarrow \bullet \rightarrow \bullet$.¹ They are of interest because they are expected to give in some sense deformation-generic models for Legendrian singularities, and for skeleta of Weinstein manifolds [11, 18, 5].

The arboreal singularities are essentially defined as cones on the above pictures. This has, at first glance, little in common with what Arnol'd would have associated to the same trees and called the A_n singularities — these being given by the singular fibers of the functions $y^2 - x^{n+1}$. Nevertheless, there is a relation. For example, one can see from the pictures that the homotopy type of the link of the depicted arboreal singularity is the same as the Milnor fibre of the A_n singularity.

Let us note another hint that the two objects should be related. Nadler calculated in [13] certain microlocal sheaf invariants associated to the arboreal singularity. On the other hand, Seidel in [16] associates to a function, such as $y^2 - x^{n+1}$, a certain category which

¹For each tree with n vertices, there are arboreal singularities of every dimension $\geq n - 1$, related by a suspension procedure. The singularity and its suspensions behave similarly, and we will not typically distinguish between them. Topologically, the link of a suspension of singularities is a suspension in the sense of topology. What are depicted here are the front of the links of: a twice suspended A_1 , a once suspended A_2 , and the most primitive model of A_3 .

can be calculated by his categorification of Picard-Lefschetz theory. Both calculations yield the same result: modules over the corresponding tree quiver.

The purpose of this note is to clarify the geometric relationship between these structures. First we must abstract from the singularity theoretic setting only the relevant symplectic geometry. A small perturbation of the function whose singularity we are studying gives a Lefschetz fibration $f : \mathbb{C}^n \rightarrow \mathbb{C}$. Recall more abstractly that to a Liouville manifold F and an ordered collection of Lagrangian spheres $S_1, \dots, S_k \subset F$, it is possible to form an exact symplectic Lefschetz fibration $X \rightarrow \mathbb{C}$ with general fibre F and vanishing cycles S_1, \dots, S_k . (Roughly speaking, to make X one takes F times a unit disk and attaches a handle along the Legendrian S_r in the fiber at $L \times e^{2\pi ir/k}$.)

In fact, we want to discard the Lefschetz fibration as well, and consider only the pair (X, F) . Technically we ask X to be the completion of a Liouville domain, with a domain completing to F contained in the contact boundary $\partial_\infty X$ of the domain completing to X . The deformation equivalence class of this pair already suffices to determine the derived Fukaya-Seidel category of the fibration [19, 6].² The geometry of such pairs is studied e.g. in [1, 19, 6, 5]. They are a symplecto-geometric version of manifolds with boundary; in particular, the cotangent bundle of a manifold with boundary yields such a pair.

Recall that to a Liouville manifold $(X, \omega = d\lambda)$ one associates the *skeleton* $\mathfrak{s}(X)$, defined to be the locus of points which do not escape under the Liouville flow. Similarly, to a Liouville pair $(X, F, \omega = d\lambda)$, one associates the *relative skeleton* $\mathfrak{s}(X, F)$, given by the locus of points in X which do not escape to $\partial_\infty X \setminus \mathfrak{s}(F)$ under the Liouville flow. Note that the skeleton and relative skeleton are *most certainly not* deformation invariants, though it is true that $\mathfrak{s}(F)$ is determined by the contact structure on $\partial_\infty X$, rather than a contact form.

For a tree T , we write Π_T for the plumbing of cotangent bundles of spheres with dual graph T . Given an ordering of the spheres, we may form the corresponding Lefschetz fibration, (X, Π_T) . Note that re-ordering the spheres in such a way that intersecting spheres – adjacent nodes of the tree – are not interchanged evidently induces an isotopy of the Lefschetz fibrations. Given a rooting \vec{T} of the tree T , we take any total order compatible with the partial order induced by the rooting; by the previous remark, these lead to isotopic Lefschetz fibrations. It is not difficult to see that the total space of this fibration is just \mathbb{R}^{2n} . We write $(\mathbb{R}^{2n}, \Pi_{\vec{T}})$ for this Liouville pair. Here we show:

Theorem 1.1. *Let \vec{T} be a rooted tree. Then $(\mathbb{R}^{2n}, \Pi_{\vec{T}})$ is deformation equivalent to a Liouville pair whose relative skeleton is the arboreal singularity associated to \vec{T} .*

Remark 1.2. As explained in [13], the arboreal link admits a cover by arboreal singularities of lower dimension, indexed by correspondences of trees. It would be interesting to

²Note that there is a difference between deformation equivalence of Lefschetz fibrations and of Liouville pairs. This is reflected in the difference between given the Fukaya-Seidel category together with a generating exceptional collection up to mutation, and just being given the category. In any case, we consider here deformation equivalence of pairs.

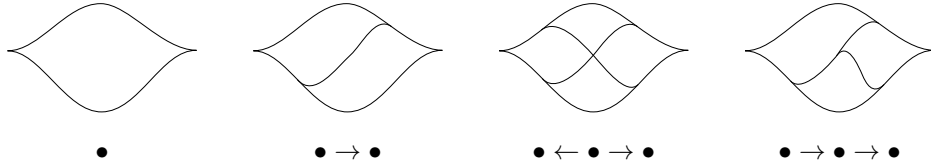


FIGURE 1. Links of the arboreal singularities for various trees.

understand how this cover and these correspondences interact with deformation to a Lefschetz fibration.

Acknowledgements. I thank Roger Casals, Yakov Eliashberg, Sheel Ganatra, Peter Lambert-Cole, Emmy Murphy, John Pardon, and Laura Starkston for helpful discussions and comments on earlier versions of this note.

Remark 1.3. Some remarks on the history of Thm 1.1. Paul Seidel noted the relationship between the arboreal link and the Milnor fiber of A_2, A_3 singularities after a talk of John Pardon, who then asked me whether such a thing might hold in general.

Thm 1.1 was announced in [6, Rem. 1.6]. Originally we planned to use it to develop properties of arboreal covers of Weinstein manifolds, both to prove that the Fukaya category cosheafifies over an arboreal skeleton, and to compare the resulting cosheaf to the one coming from microlocal sheaf theory [9, 12, 17]. Since this time, our strategy to prove the cosheaf property has evolved so as not to require arborealization (see [7, Thm. 1.20] for a representative special case) and in addition due to [8] (and [17, 14]) we no longer require any special form for the skeleton to make the local identification with the sheaf category. In particular, this result is no longer necessary for that programme.

Of course, the deformation-genericity of arboreal singularities means they are of interest far beyond their role in categorical calculations. Perhaps the above result may clarify the nature of these objects. At the least it decreases the cognitive dissonance caused by the fact that after [13], the term “ A_n singularity” acquired more than one meaning.

2. Some singular Legendrians

We typically write \vec{T} to mean a rooted tree. If v is any vertex of the tree, we write $\vec{T}(v)$ for the sub-tree growing from v (trees grow away from the root).

By a *shrub* we mean a tree with all vertices at distance at most one from the root. We write $\vec{T}_{\leq 1}(v)$ for the shrub growing from a given vertex.

By a singular Legendrian, we mean a finite union of isotropic submanifolds which is the closure of its smooth Legendrian locus. Here we present three different families of singular Legendrians associated to rooted trees; we define them inductively just by drawing fronts.

2.1. Arboreal singularities

Definition 2.1. Let \vec{T} be a rooted tree, and fix $n \geq |\vec{T}| - 1$. We will define the *arboreal link* corresponding to \vec{T} as a certain explicit Legendrian by giving a front projection to \mathbb{R}^n . The construction is recursive in nature. We assume $n \geq 2$.

We take the first $|\vec{T}| - 1$ coordinates of \mathbb{R}^n to be indexed by the non-root vertices of the tree. In front projections, one direction is distinguished (“no vertical tangencies”); we take the vertical direction to be given by the sum of the coordinates.

Everything is built from the front associated to $\bullet \rightarrow \bullet$ in Figure 1. Note that the diagonal line dividing the big unknot is, away from the big unknot, a disk in a coordinate axis (recall that our coordinate hyperplanes are always slanted). The choice of coordinates is such that this axis is the one on which the leaf vertex coordinate vanishes.

For shrubs the construction is as follows. Take the front for $\bullet \rightarrow \bullet$, and suspend it appropriately so it becomes a front in the desired dimension. Now it is a big unknot (saucer) with a slice through the middle, which is mostly just a disk in a coordinate hyperplane. By permuting coordinates, this could be any coordinate hyperplane. The desired front is obtained by taking the union the fronts corresponding to the hyperplanes named by the non-root vertices. For an example when $n = 2$, see the front associated to $\bullet \leftarrow \bullet \rightarrow \bullet$ in Figure 1.

In general we proceed as follows. First apply the above construction to the shrub obtained from pruning all vertices of distance > 1 from the root. Now, for each vertex v which is one away from the root, re-focus attention on the unknot bounded by (the lower) half the original unknot plus the hypersurface associated to v . Working inside this new unknot, apply the algorithm to the tree $\vec{T}(v)$ which grows from v .

The careful reader may have noticed that the unknot we used for the second and later steps of the algorithm is singular – it has a corner where the middle piece meets the original unknot. Said reader may convince themselves that this leads to no ambiguity in the description. One possibility is to make even the original unknot singular, e.g. by drawing the (non-generic) front as a cube stood on its corner. \triangle

Remark 2.2. Nadler originally introduced the arboreal singularities as Legendrian singularities. We have described the Legendrian link of the Lagrangian projection of this entity.

2.2. Armadillos

Definition 2.3. Let \vec{T} be a rooted tree. Extend the partial order on the vertices of \vec{T} coming from the tree structure to a total order. From this data we define a front recursively as follows.

To the shrub growing from the root, we associate the picture in Figure 2. This figure contains the front of a large unknot, and several smaller ones which are tangent to it with a simple tangency.

Here the smaller unknots are ordered left to right matching the total ordering of the vertices. The full picture associated to \vec{T} is given by now recursively applying this con-

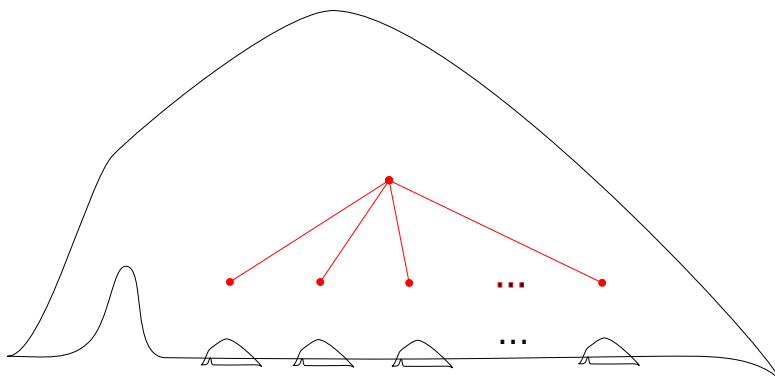


FIGURE 2. The armadillo of a shrub.

struction to the trees which grow from the vertices at distance one from the root, except now using the depicted small unknots as the big unknot. \triangle

The corresponding Legendrian is the skeleton of a collection of cotangent bundles of spheres plumbed according to the diagram T . Evidently, up to ambient isotopy, it does not depend on the details of the way Figure 2 was drawn. (Below we will recall from [3] a more abstract meaning of the symplectic geometry of the particular Legendrian embedding of the skeleton of the plumbing determined by the armadillo front diagram.)

Remark 2.4. The picture is in a two dimensional front plane, but evidently this prescription makes sense for any number of dimensions $n \geq 2$. Note that (up to a non-contractible space of isotopies) the total ordering of the vertices of \vec{T} becomes irrelevant in higher dimension.

2.3. Motherships

It will be convenient to interpolate between the arboreal singularities and the armadillos by introducing another class of singular Legendrians indexed by trees. As before, we give an inductive definition.

Definition 2.5. (motherships) Let \vec{T} be a rooted tree. Extend the partial order on the vertices of \vec{T} coming from the tree structure to a total order. From this data we define a front recursively as follows.

To the shrub growing from the root, we associate the picture in Figure 3. Here the smaller unknots are ordered left to right matching the total ordering of the vertices. The full picture associated to \vec{T} is given by now recursively applying this construction to the trees which grow from the vertices at distance one from the root, except now using the depicted small unknots as the big unknot. \triangle

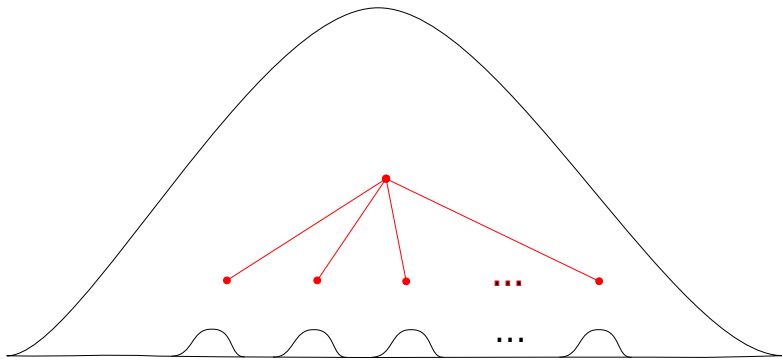


FIGURE 3. The mothership of a shrub.

Remark 2.6. In order that the big unknot have exactly the same front as the small unknots, it must be taken to be singular as a Legendrian above its cusps.

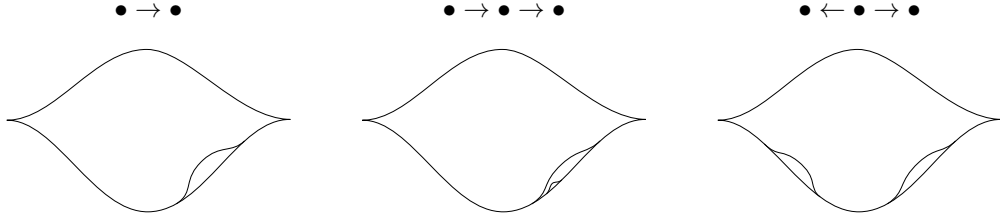
The total ordering of branches becomes irrelevant in front dimension ≥ 2 . In higher dimensions, it will be convenient to have a variant where the loci of attaching smaller saucers is prescribed in a way more similar to the description of the arboreal link.

Definition 2.7. (coordinated motherships) Let \vec{T} be a rooted tree, and choose some $n \geq |\vec{T}| - 1$. We will draw a front in \mathbb{R}^n . As for the arboreal singularity, non-root vertices of the tree index coordinates of \mathbb{R}^n (excess coordinates go unindexed) and the vertical direction is the sum of the coordinates.

Begin with the front of a flying saucer, centered about the origin. The bottom half of the saucer projects vertically to a disk of some fixed radius in the plane $\sum x_i = 0$; correspondingly I will use the x_i as coordinates on this bottom half (subject to the condition that they sum to zero). Inscribe a simplex of the same dimension in this disk, with the facets being given by setting some coordinate to a constant value. Mark a point at the center of each facet.

In short, there are now n marked points on the bottom of the flying saucer, one for each coordinate. For each of these which corresponds to a vertex of the tree with distance one from the root, take a small disk around it, and use it as the base for a (singular) saucer. (The top should be a disk of the same size).

Now recursively apply this algorithm for the trees growing from the vertices at distance one for the root, in each case replacing the original big saucer with the small one that was created in the previous step. \triangle

FIGURE 4. Coordinated motherships for $n = 2$.

3. Ribbons

3.1. Generalities

Definition 3.1. Let V be contact and $\Lambda \subset V$ be a singular Legendrian. A *ribbon* for Λ is a codimension one submanifold $R \subset V$ such that some local contact form near λ determines a Liouville structure on R with skeleton Λ . \triangle

We have the following standard facts:

Lemma 3.2. *The Reeb vector field is transverse to any ribbon*

Proof. Recall by definition the Reeb vector field is in the kernel of $d\lambda$. Since $d\lambda|_R$ is nondegenerate, the Reeb field cannot be tangent to R at any point, thus is transverse to R . \square

Lemma 3.3. *A ribbon determines a contact embedding of (an neighborhood of R in the) contactization $R \times \mathbb{R} \rightarrow V$ carrying the skeleton of R to \mathbb{L} .*

Proof. Pushing by Reeb sweeps out the desired embedding. \square

We *do not* know whether any two ribbons are isotopic. It is however possible to show the following, which already implies that no Floer theoretic invariants will depend on the choice of the ribbon.

Lemma 3.4. *Given any two ribbons R, S for the same Legendrian, one can find ribbons R', R'' isotopic as ribbons to R , such that $R' \subset S \subset R''$ and the inclusion $R' \subset R''$ is trivial (i.e. the Liouville flow on R'' gives an isotopy between them).*

Proof. The point is that R and S must both have tangent spaces transverse to the Reeb flow along the skeleton, hence in a small neighborhood thereof, each will be graphical over the other in the aforementioned embedding of the contactization. \square

Remark 3.5. We say that the ribbon of a singular Legendrian is unique up to matryoshka.

A fundamental question is:

Question 3.6. Which singular Legendrians admit a ribbon?

There are evident local obstructions (an example of John Pardon: take many smooth Legendrian curves with varying second order behavior through a point; no surface can contain them all). We do not know whether there are global obstructions.

The situation is of course even worse for the family version:

Question 3.7. When does a family of singular Legendrians arise as the family of cores of an isotopy of ribbons?

Definition 3.8. We say a 1-parameter family of singular Legendrians which arises as the family of cores of an isotopy of ribbons is a *ribbotopy*.³ \triangle

Given a ribbon, two things we can do to construct a family of ribbons are the following. One is to apply an ambient contact isotopy. The other is to apply a contact contact isotopy along a contact level of the ribbon itself:

Lemma 3.9. [4] *Let (R, λ) be a Liouville domain and $R^{in} \subset R$ a subdomain. Then from a contact isotopy $\phi_t : \partial R^{in} \rightarrow \partial R^{in}$ one can construct a 1-parameter family λ_t of Liouville forms such that the Liouville flow is unchanged away from a collar neighborhood of ∂R^{in} , and integrates to ϕ_t when traveling across this neighborhood.*

The ribbotopies we use will be of the following form. Given some contact manifold (V, λ) and Liouville hypersurface R , we will cut R into R^{in} and $R^{out} = R \setminus R^{in}$. We push R^{out} by an ambient contact isotopy which restricts to a contact isotopy along ∂R^{in} . That is, from the point of view of the 1-form on the family of hypersurfaces thusly created, the isotopy looks like that of the above lemma. (Below, the R^{out} will always be the part corresponding what is further towards the leaves of the tree.)

3.2. Graph ribbotopies

The notions of ribbon and ribbon equivalence are well studied in the context of Legendrian graphs in contact 3-manifolds. Many explicit diagrams of isotopies and ribbotopies can be found e.g. in the papers [2, 15, 10]. In Figure 5 we collect the graph ribbotopies. They allow a sanity check on the later alleged ribbotopies by drawing them in this dimension as a sequence of these moves. Almost all moves we require can be obtained as stabilizations of these moves.⁴

It is useful to note that a Legendrian graph has, at each vertex, a canonical cyclic order of the edges, since all their tangents must lie in the contact plane. What is going on in the ‘C’ moves is just that a given edge is sliding onto an edge either immediately before

³It moves the ribs of the skeleton.

⁴The only exception is the main construction of Section 4.3, which in turn is an exception only in that the move there does not admit a front projection which is locally a graph ribbotopy times \mathbb{R}^n , for the reason that other unrelated components will appear in the front projection, whose Legendrian lifts however remain disjoint from the ribbotopy.

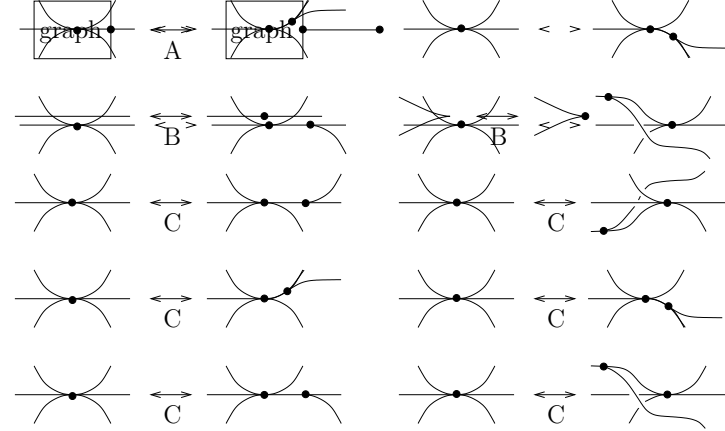


FIGURE 5. Graph ribbonotopies (from [2]).

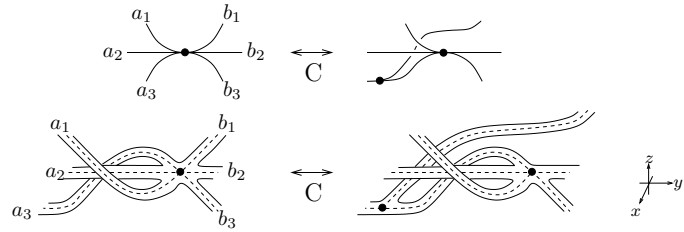


FIGURE 6. The 'C' moves are a bit weird from the point of view of the front projection. It is clearer when the surface is drawn. (from [2]).

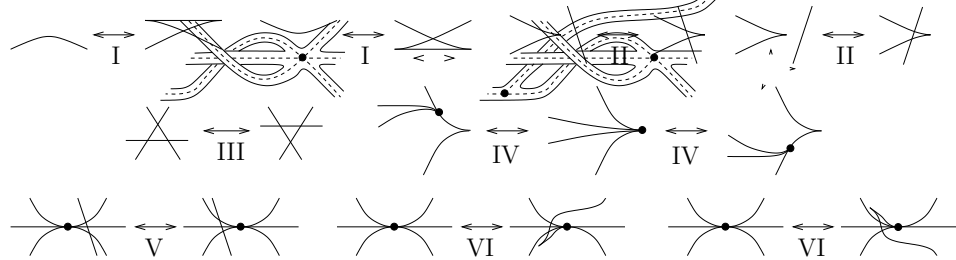


FIGURE 7. The Reidemeister moves for graphs (from [2]).

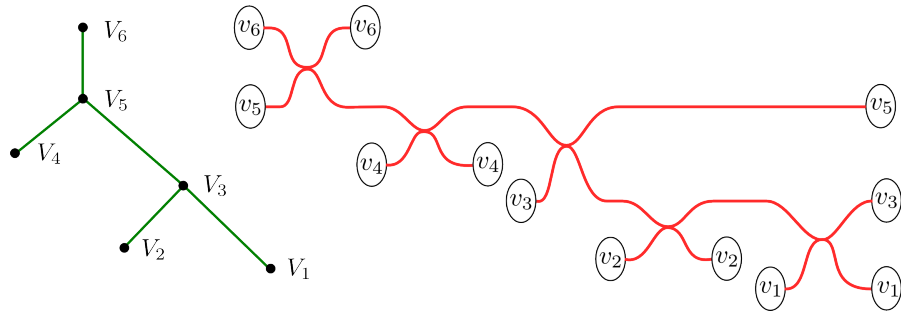


FIGURE 8. The front of a plumbing, as drawn in the front space for \mathbb{R}^{2n} after attaching several subcritical handles. (From [3].)

or immediately after it in the cyclic order. The apparent weirdness of the ‘C’ moves has to do with the fact that the cyclic order is messed up by the front projection. In the front projection, the cyclic order is: negative-to-positive slopes to the right of the vertex, then positive-to-negative slopes to the left of the vertex.

Also useful will be the Reidemeister moves for Legendrian graphs, i.e., ways the front projection can be altered by a small contact isotopy. These are again from [2]. We will frequently draw move VI; a good way to think of it is as half of a Reidemeister 1 move.

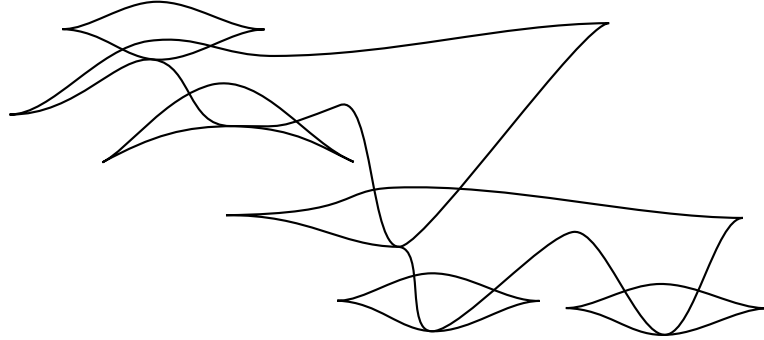
4. Proof of Theorem 1.1

We will show in Section 4.1 that the plumbings have link given by the armadillo; in Section 4.2 that the armadillo is ribbotopic to the mothership, and in Section 4.3 that the arboreal link is ribbotopic to the coordinated mothership. The coordinated mothership being obviously ribbotopic to the mothership, this will complete the proof of Theorem 1.1.

4.1. The relative skeleton of $(\mathbb{R}^{2n}, \Pi_{\vec{T}})$

In [3], an algorithm is given for drawing front projections of Legendrians which live in the boundaries of Lefschetz fibrations whose fibre is a sphere plumbing. We only need the zeroeth step of this algorithm: drawing the front projection of the skeleton of the plumbing itself. In [3], the Legendrians of interest are in the contact manifold $\partial(\Pi_{\vec{T}} \times \mathbb{C})$. This contact manifold is obtained from S^{2n-1} by attaching (subcritical) handles along a certain amount of S^{n-2} . Thus they draw fronts in an \mathbb{R}^n with a certain amount of S^{n-2} ’s indicating the attaching spheres for the handles. They give explicitly a picture of the skeleton of the plumbing in this space. See Figure 8.

We are interested in understanding this skeleton in a different space: the contact boundary of the Weinstein manifold which results from cancelling these S^{n-2} ’s with

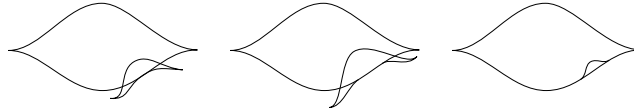
FIGURE 9. The front of a plumbing, as drawn in the front space for \mathbb{R}^{2n} .

critical handles, which should be attached along the S^{n-1} 's which are plumbed together to make the skeleton. The front projection of the result is given by erasing the attaching sphere loci, adding a small (say upwards) pushoff of each of these D^{n-1} 's which are visible in the projection, then connecting them to the one below to make a flying saucer. The result is isotopic to the armadillo of Def. 2.3. See Figure 9. We conclude:

Proposition 4.1. *Let \vec{T} be a rooted tree. Consider the Liouville pair $(\mathbb{R}^{2n}, \Pi_{\vec{T}})$ arising from the Lefschetz fibration with fibre the plumbing of sphere cotangent bundles $\Pi_{\vec{T}}$ and vanishing cycles the ordered zero sections. Then $\mathfrak{s}(\mathbb{R}^{2n}, \Pi_{\vec{T}})$ is carried by an ambient contact isotopy to the Legendrian with front as in Def. 2.3.*

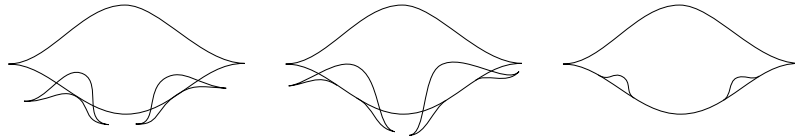
4.2. Armadillos to motherships

The basic move to turn an armadillo into a mothership is



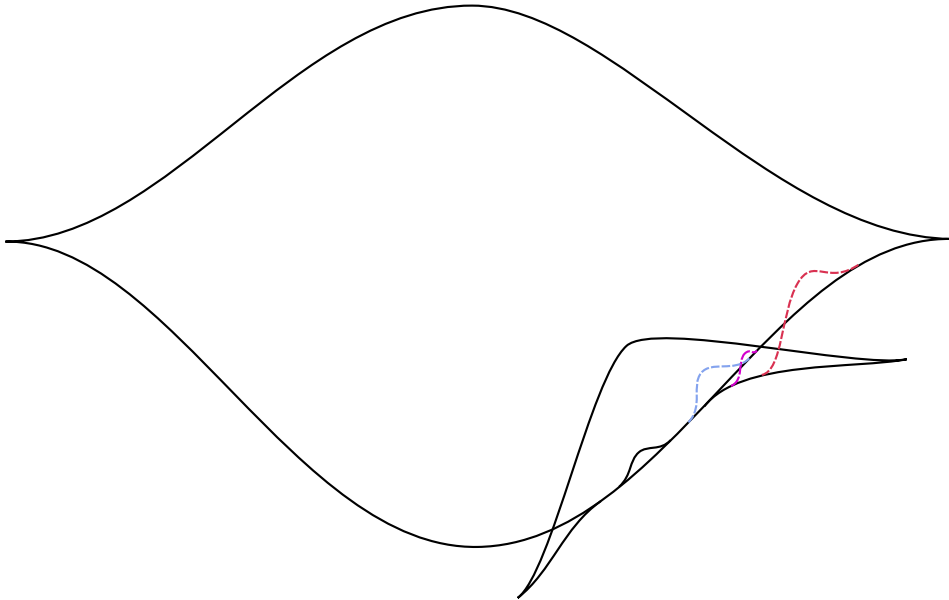
The first step is a nontrivial ribbotopy, the second is just an isotopy (in this dimension, the first step is the type 'C' ribbotopy in the list above, and the second is the type 'VI' Reidemeister move. Evidently this works for shrubs, in any dimension.

Example 4.2. For $\bullet \leftarrow \bullet \rightarrow \bullet$:

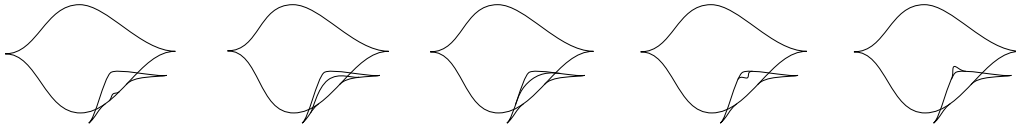


To set up the inductive procedure one runs into the following difficulty. Try to apply the above move starting from the mothership for $\bullet \rightarrow \bullet \rightarrow \bullet$. There is no difficulty for the middle ‘pod’ corresponding to the central \bullet . However after transforming this one, the smallest unknot is preventing the middle sized unknot from contracting the edge it shares with the largest unknot. So one has to get the small unknot out of the way; also in the end it should share an edge with only the middle unknot and not touch the large one at all.

One can try to just push the smallest pod e.g. to the right. However, attempting to do this has the following undesirable result:



Instead we do the following:

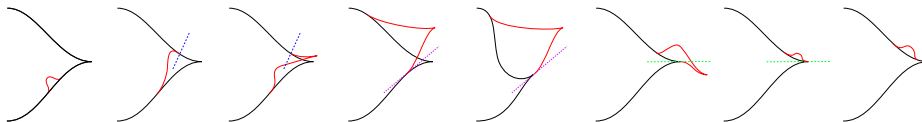


In the first four pictures, the smaller unknot is travelling along the medium unknot; the junction where they meet is moving by the cone on the Reeb flow nearby. The passage from the first picture to the second is a ribbotopy, and from the second to the fourth, just isotopy. The fourth to the fifth is a ribbotopy: the bottom piece of the smallest unknot becomes part of the medium unknot, and the top piece of the smallest unknot (previously also a piece of the medium unknot) moves up.

Note this works in any dimension, and with any number of smallest nested unknots. Indeed, consider where they attach to the medium unknot. The dynamics of these spheres is that of the fronts of waves emitted simultaneously from several points on the sphere. The legendrians of these waves never meet each other (after all they are all flowing by Reeb), and eventually the reconverge at the antipodal points.

In the case that there are further levels of nesting, this procedure should be applied to the lowest (further from the root) nested level first. Now the smaller levels have gotten out of the way, it is possible to ribbotope the unknots corresponding to the nodes one away in the tree to look like the plumbing model.

Note there is an ambient isotopy carrying the higher nested unknots living at the top back down to the bottom. Here is a picture in front projections, communicated to me by Peter Lambert-Cole. The dashed lines indicate that a VI move is about to (or has just) been performed, and they are the “horizontal” lines with respect to this move.

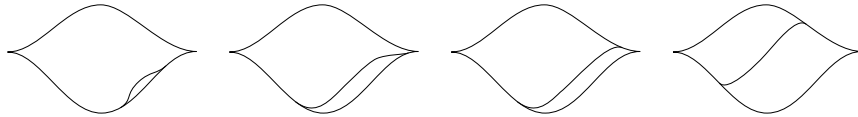


4.3. Arboreal links to motherships

The idea is as follows: each hypersurface we have introduced in making the front diagram for the arboreal link is mostly a coordinate hypersurface. We slide all these hypersurfaces simultaneously along their normal direction which points downward (recall that the vertical axis is the sum of the coordinates). A hypersurface corresponding to a vertex on the k 'th level of the tree should slide at speed c^{-k} for some constant $c > 1$.

To define it more precisely, we proceed as usual to first define it for the tree $\bullet \rightarrow \bullet$, then extend to shrubs, and finally to extend to all trees by induction.

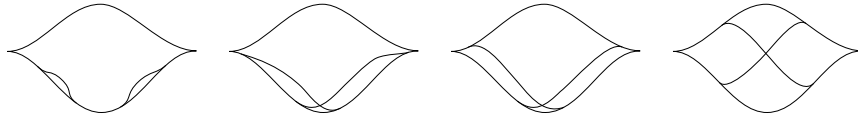
The picture for $\bullet \rightarrow \bullet$ is:



This is just an isotopy. (In terms of the Reidemeister moves above, we used move IV.)

As usual, for shrubs we suspend the picture and take a union over appropriate permutations of coordinates. Away from the big unknot, this is still an isotopy: the hypersurfaces meet in the front projection, but where they meet they are parallel to distinct coordinate hypersurfaces, hence have different lifts. Near the big unknot, it is not an isotopy – the loci where the hypersurfaces meet the big unknot will meet during the movie – but the behavior along the big unknot is a cone of the nearby behavior, hence is a ribbotopy.

Example 4.3. Scenes from the movie for $\bullet \leftarrow \bullet \rightarrow \bullet$:

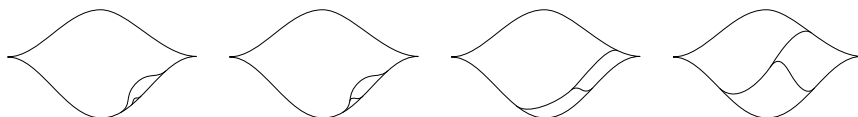


All the action happens between the first scene and the second. This is a ribbotopy of type ‘C’ in the list above.

We turn to the general case. In the front projection, the root node corresponds to the outermost unknot. The immediate children of the root node each correspond to an unknot front sharing the lower component with the root unknot. We will term these the ‘pods’. Fixing attention on these pods, by induction we find for each a local ribbotopy changing the legendrian such that only the front projection within each pod is changing, and within each pod the mothership picture is replaced by the corresponding arboreal picture. Finally, apply to the upper boundaries of the pods the same ribbotopy as described in the shrub case.

One must check that whatever is going on in the interior of the pods does not interfere with the moving hypersurfaces in this last step. This is true because inside the pods we have the arboreal configuration, i.e. all components are approximately conormal to some coordinate hyperplane, and no coordinate hyperplane occurs more than once. So away from the big unknot, the moving fronts of these hypersurfaces lift to disjoint legendrians. This extends to the big unknot as a ribbotopy.

Example 4.4. $\bullet \rightarrow \bullet \rightarrow \bullet$.



Again, the movie is just an isotopy except between the first scene and the second.

References

- [1] R. Avdek. *Liouville hypersurfaces and connect sum cobordisms*. ArXiv Preprint, arXiv:1204.3145:1–58, (2012).
- [2] S. Baader and M. Ishikawa. *Legendrian graphs and quasipositive diagrams*. ArXiv Preprint, math/0609592:1–17, (2006).
- [3] R. Casals and E. Murphy. *Legendrian fronts for affine varieties*. Duke Mathematical Journal, **168**(2):225–323, (2019).
- [4] K. Cieliebak and Y. Eliashberg. *From Stein to Weinstein and back: symplectic geometry of affine complex manifolds*, American Mathematical Society Colloquium Publications. American Mathematical Society, Providence, RI, (2012).
- [5] Y. Eliashberg. *Weinstein manifolds revisited*. Arxiv Preprint, arXiv:1707.03442v2:1–32, (2017).
- [6] S. Ganatra, J. Pardon, and V. Shende. *Covariantly functorial wrapped Floer theory on Liouville sectors*. Pub. Math. IHES, **131**:73–200, (2020).
- [7] S. Ganatra, J. Pardon, and V. Shende. *Sectorial descent for wrapped Fukaya categories*. ArXiv Preprint, arXiv:1809.03427v2:1–111, (2018).
- [8] S. Ganatra, J. Pardon, and V. Shende. *Microlocal Morse theory of wrapped Fukaya categories*. ArXiv Preprint, arXiv:1809.08807:1–47, (2018).
- [9] M. Kashiwara and P. Schapira. *Sheaves on manifolds*, Grundlehren der Mathematischen Wissenschaften [Fundamental Principles of Mathematical Sciences]. Springer-Verlag, Berlin, (1990). With a chapter in French by Christian Houzel.
- [10] P. Lambert-Cole and D. O’Donnol. *Planar Legendrian graphs*. ArXiv Preprint, arXiv:1604.00836:1–23, (2016).
- [11] D. Nadler. *Non-characteristic expansions of Legendrian singularities*. ArXiv Preprint, arXiv:1507.01513:1–47, (2016).
- [12] D. Nadler. *Wrapped microlocal sheaves on pairs of pants*. Arxiv Preprint, arXiv:1604.00114:1–50, (2016).
- [13] D. Nadler. *Arboreal singularities*. Geom. Topol., **21**(2):1231–1274, (2017).
- [14] D. Nadler and V. Shende. *Sheaf quantization in Weinstein symplectic manifolds*. Arxiv Preprint, arXiv:2007.10154:1–59, (2020).
- [15] D. O’Donnol and E. Pavelescu. *On Legendrian graphs*. Algebr. Geom. Topol., **12**(3):1273–1299, (2012).
- [16] P. Seidel. *Fukaya categories and Picard-Lefschetz theory*. Zurich Lectures in Advanced Mathematics. European Mathematical Society (EMS), Zürich, (2008).
- [17] V. Shende. *Microlocal category for Weinstein manifolds via h-principle*. ArXiv Preprint, arXiv:1707.07663:1–6, (2017).
- [18] L. Starkston. *Arboreal singularities in Weinstein skeleta*. Selecta Mathematica, **24**:4105–4140, (2018).
- [19] Z. Sylvan. *On partially wrapped Fukaya categories*. Journal of Topology, **12**(2):372–441, (2019).

UC BERKELEY, MATH DEPT. 873 EVANS HALL SAN FRANCISCO
Email address: vivek@math.berkeley.edu